Tapio Salmi, Jyrki Kuusisto, Johan Wärnå, Jyri-Pekka Mikkola
Åbo Akademi, Process Chemistry Centre
FI-20500 Turku/Åbo, Finland
tsalmi@abo.fi

ALTERNATIVE SWEETENERS: LA DOLCE VITA

Catalytic production of sweeteners from natural sources was considered: three-phase hydrogenation of *D*-fructose, *D*-xylose and *D*-lactose. Mathematical modelling including reaction, mass transfer and catalyst deactivation was successfully applied.

A typical way to produce alternative sweeteners is to hydrogenate an aldehyde or a ketose to the corresponding polyol, such as catalytic hydrogenation of *D*-xylose to xylitol, *D*-fructose to mannitol/sorbitol and *D*-lactose to lactitol. On paper, these reactions are simple, and they can schematically be written as:

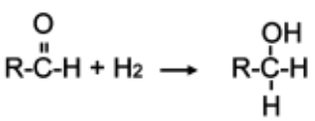

However, the pattern is complicated by several factors. The sugar molecules to be hydrogenated mutarotate in aqueous solutions thus co-existing as acyclic aldehydes and ketoses and as cyclic pyranoses and furanoses, reaction kinetics are complicated and involve side reactions, such as isomerization, hydrolysis and oxidative dehydrogenation reactions. Moreover, catalysts deactivate and, last but not least, external and internal mass transfer limitations might interfere with the kinetics, particularly under industrial circumstances.

Several solid catalysts have been studied, depending on the particular process. For instance, for hydrogenation of xylose and lactose, various Ni and Ru catalysts work well, while Cu based catalysts give high mannitol selectivity in the hydrogenation of fructose. Catalytic hydrogenation is typically carried out in slurry reactors, where finely dispersed catalyst particles (<100 μm) are immersed in a dispersion of gas and liquid. It has, however, been demonstrated that continuous operation is possible, either by using trickle bed [1] or monolith technologies. Elevated pressures and temperatures are needed to have a high enough reaction rate. On the other hand, too high a temperature impairs the selectivity of the desired product, as has

Devoted to prof. Elio Santacesaria in honour of his 65th birthday and of his constant contribution to innovative new processes development in industrial chemistry.

Table - Processes and catalysts for production of artificial sweeteners

Educt	Product	Catalyst	Conditions
Fructose	Mannitol Sorbitol	sponge Ni, Cu	100-130 °C, >40 bar
Glucose	Sorbitol	Ru, sponge Ni	100-130 °C, >40 bar
Lactose	Lactitol	sponge Ni, Ru	110-120 °C, >40 bar
Xylose	Xylitol	sponge Ni, Ru	100-120 °C, >40 bar

been demonstrated by Kuusisto *et al.* [2]. An overview of some feasible processes and catalysts is provided by Table above.

In any case, a rational scale up of a production process should be based on correct stoichiometric and kinetic model, as discussed by many authors [3, 4]. Moreover, kinetics is exciting *per se*, since it yields valuable information about the underlying reaction mechanisms [5]. Thus it is very important that the kinetic information is not obscured by catalyst deactivation and mass transfer effects. To obtain correct stoichiometric information is a challenge itself in case of artificial sweeteners, since by-products typically appear in low concentrations (below 1 weight-%) in concentrated environment (the concentrations of reactant and main product being typically 20-60 weight-%). Thus very precise high-pressure liquid chromatography (HPLC) is typically used, and the work is completed with NMR-analysis [6].

Internal and external mass transfer limitations in porous catalyst layers play a central role in three-phase processes. The governing phenomena are well-known since the days of Thiele [7] and Frank-Kamenetskii [8], but transport phenomena coupled to chemical reactions is not frequently used for complex organic systems, but simple - often too simple - tests based on the use of first-order Thiele modulus and Biot number are used. Instead, complete numerical simulations are preferable to reveal the role of mass and heat transfer at the phase boundaries and inside the porous catalyst particles.

In the presence of organic components, catalyst deactivation due to poisoning and fouling retard the activity and suppress the selectivity with time. At elevated reaction temperatures, sintering of the catalyst can take place. Thus it is important to obtain reliable models for catalyst deactivation and to investigate, whether it is possible to decouple the deactivation model from the kinetic model or is it necessary to treat the catalyst deactivation as one of the surface reactions on the catalyst [9]. Production of artificial sweeteners is often carried out in batch and semi-batch reactors, which imply that time-dependent, dynamic models are required to obtain a realistic description of the process.

In the current paper, we demonstrate the pathway from stoichiometric and kinetic studies to investigation of catalyst deactivation and transport phenomena. By applying systematic experimentation and mathematical modeling, the manufacture of sweeteners becomes *la dolce vita* with growing industrial interest.

Modelling porous catalyst particles

Reaction, diffusion and catalyst deactivation in porous particles is considered. A general model for mass transfer and reaction in a porous particle with an arbitrary geometry can be written as follows:

$$\frac{dc_i}{dt} = \varepsilon_p^{-1}\left(r_i \rho_p - r^s \frac{d\left(N_i r^s\right)}{dr}\right) \qquad (1)$$

where the component generation rate (r_i) is calculated from the reaction stoichiometry

$$r_i = \sum_j \nu_{ij} R_j a_j \qquad (2)$$

where R_j is the initial rate of reaction j and a_j is the corresponding activity factor.

The catalyst activity factor (a_j) is time-dependent. Several models have been proposed in the literature, depending on the origin of catalyst deactivation, i.e. sintering, fouling or poisoning (8). The following differential equation can represent semi-empirically different kinds of separable deactivation functions

$$\frac{da_j}{dt} = -k_j'\left(a_j - a_j^*\right)^n \qquad (3)$$

where k_j' is the deactivation parameter and a_j' is the asymptotic value of the activity factor - for irreversible deactivation, $a_j^*=0$. Depending on the value of the exponent (n), the solution of eq. (3) becomes

$$a_j = a_j^* + \left(a_{0j} - a_j^*\right)e^{-k_j t} \qquad (4a)$$

and

$$a_j = a_j^* + \left(\left(a_0 - a_*\right)^{n-1} k_j'(n-1)t\right)^{\frac{1}{n-1}},\ n \neq 1 \qquad (4b)$$

Some special cases of eq. (4) are of interest: for irreversible first

(n=1) and second (n=2) order deactivation kinetics we get $a_j = a_{0j}e^{-k_j t}$ and $a_j = a_{0j}/(1 + a_{0j}k'_j t)$ respectively.

In case that the effective diffusion coefficient approach is used for the molar flux, it is given by $N_i = -D_{ei}(dc_i/dr)$, where $D_{ei}=(\varepsilon_p/\tau_p)D_{mi}$ according to the random pore model. A further development of eq. (1) yields

$$\frac{dc_i}{dt} = \varepsilon_p^{-1}\left(\rho_p \sum \nu_{ij} R_j a_j + D_{ei}\left(\frac{d^2 c_i}{dr^2} + \frac{s}{r}\frac{dc_i}{dr}\right)\right) \quad (5)$$

The boundary conditions of eq. (5) are

$$\frac{dc_i}{dr} = 0 \quad (6a)$$

at r = 0 and

$$D_{ei}\left(\frac{dc_i}{dt}\right)_{r=R} = k_{Li}\left(c_i - c_i(R)\right) \quad (6b)$$

at r = R, where c_i is the bulk-phase concentration of the component. The initial condition at t=0 is $c_i(r)=ci$, i.e. equal to the bulk-phase concentration.

The molecular diffusion coefficients in liquid phase were estimated from the correlations Wilke and Chang [10] for organic solutions and Hayduk and Minhas [11] for aqueous solutions, respectively. The solvent viscosities needed in the correlations were obtained from the empirical equation based on the experimental data, $\ln(\eta/cP) = A + B/T$, where the parameters A and B are experimentally determined constants. Spherical particles (s=2), were used in the experiments. Hydrogen solubility in the organic reaction mixture was obtained from correlation of Fogg and Gerrard [12], $\ln(x^*_{H_2}) = A + B/T$, where $x^*_{H_2}$ is the mole fraction of dissolved hydrogen in equilibrium, and A and B are experimentally determined constants. For aqueous sugar solutions, a correlation equation proposed by Mikkola *et al.* [13] was used.

The liquid-solid mass transfer coefficient was estimated from the correlation provided by Temkin *et al.* [14]. The method is based on the estimation of Sherwood number (Sh), starting from Reynolds (Re) and Schmidt (Sc) numbers

$$Sh_i = a\,\mathrm{Re}^{\alpha}\, Sc_i^{\beta} \quad (7)$$

where $Sh=k_{Li}d_p/D$. Reynolds number is calculated by using the turbulence theory of Kolmogoroff

$$\mathrm{Re}_d = \left(\frac{\varepsilon d}{\nu^3}\right)^{1/3} \quad (8)$$

and Schmidt number is defined as $Sc=\nu/D$. The experiments of Hájek and Murzin [15] have shown that the dissipated energy can in many cases be clearly less than the energy imposed by the stirrer of a slurry reactor. An analogous approach was applied on the calculation of the gas-liquid mass transfer coefficient of hydrogen (k_{LH}).

Catalytic reactor model

For a semi-batch stirred tank reactor, the model was based on the following assumptions: the reactor is well agitated, so no concentration differences appear in the bulk of the liquid; gas-liquid and liquid-solid mass transfer resistances can prevail; and finally, the liquid phase is in batch, while hydrogen is continuously fed into the reactor. The hydrogen pressure is maintained constant. The liquid and gas volumes inside the reactor vessel can be regarded as constant, since the changes of the fluid properties due to reaction are minor. The total pressure of the gas phase (P) as well as the reactor temperature were continuously monitored and stored on a PC. The partial pressure of hydrogen (p_{H2}) was calculated from the vapour pressure of the solvent (p^{VP}) obtained from Antoinès equation (p^{VP0}) and Raoult's law:

$$p^{VP} = p^{Vp0} x_{solvent} \quad (9)$$

The volatilities of the reactive organic components were negligible under the actual experimental conditions.

A general mass balance for an arbitrary liquid-phase component in the stirred tank reactor is thus written as follows

$$N_i A_p = N_{GLi} A_{GL} + \frac{dn_i}{dt} \quad (10)$$

i.e. the fluxes (N_i, N_{GLi}) negative for reactants but positive for products. Introduction of the liquid-phase concentration ($n_i=c_iV_L$), assuming a constant liquid-phase volume, and introducing the quantities $a_P=A_P/V_L$ and $a_{GL}=A_{GL}/V_L$ gives after some rearrangement:

$$\frac{dc_i}{dt} = N_i a_p - N_{GLi} a_{GL} \quad (11)$$

The initial condition is $c_i=c_i(0)$ at t=0. The flux at the particle surface is given by (see eq. 6b)

$$N_i = k_{Li}\left(c_i - c_i(R)\right) \quad (12)$$

while the flux at the gas-liquid interface is estimated from the two-

film theory resulting in the expression

$$N_{GLi} = \frac{c_{Gi}^b - K_i c_{Li}^b}{\frac{K_i}{k_{Li}} - \frac{1}{k_{Gi}}} \qquad (13)$$

In the actual case, this expression is used for hydrogen only, since the volatilities of organic reactants and products were negligible, and thus $N_{GLi}=0$ for the organics.

The concentration of hydrogen in gas phase was obtained from the ideal gas law, $c_{H_2}=p_{H_2}/(RT)$, and the equilibrium ratio of hydrogen (K_{H2}) was calculated from the equilibrium solubility ($x^*_{H_2}$, [12]) and Henry's law:

$$K_{H_2} = \frac{p_{H_2}}{x^*_{H_2} c_{TOT,L} RT} \qquad (14)$$

where $C_{TOT,L}=r_L/M_L$.

The partial differential equations describing the catalyst particle were discretized with central finite difference formulae with respect to the spatial coordinate. Typically about 9 discretization points were used for the particle. The ordinary differential equations (ODEs) created were solved with respect to time together with the ODEs of the bulk phase. Since the system is stiff, the computer code of Hindmarsh [16] was used as the ODE solver. In general, the simulations progressed without numerical troubles.

Alternative sweeteners: stoichiometry, kinetics, deactivation and mass transfer

The cases considered here are hydrogenation of fructose, xylose and lactose on various heterogeneous catalysts. The complete reaction schemes, which incorporate simultaneous, consecutive-competitive reactions, are displayed in Fig. 1.

Kinetic experiments were carried out isothermally in autoclave reactors of sizes 300 ml and 600 ml. The stirring rate was typically 1800 rpm. In most cases, the reactors operated as slurry reactors with small catalyst particles (45-90 μm), but comparative experiments were carried out with a static basket using large catalyst pellets. HPLC analysis was applied for product analysis. The experimental details are reported in previous papers of our group, e.g. by [2, 6, 13].

Product distribution analysis - stoichiometry

Preliminary product distribution plots were prepared based on experimental data representing intrinsic kinetics. The following facts were revealed from lactose hydrogenation: the dominant main product on Ni- and Ru catalysts is lactitol, while some lactulose and lactitulitol are formed through a consecutive route. In addition, formation of sorbitol and galactitol was noticed. They can principally originate either from a hydrolysis-hydrogenation route of lactose (lactose gives glucose and galactose which are hydrogenated to sorbitol and galactitol) or from hydrolysis of lactitol. After a very precise HPLC analysis, lactobionic acid was detected, but it was partially hydrogenated away. For xylose hydrogenation on Ni and Ru, the picture was simpler: the main product was xylitol, but in the lack of hydrogen, considerable amounts of the isomerization product, xylulose was formed, which was further hydrogenated to arabinitol and xylitol. For fructose hydrogenation on Cu based catalysts, a parallel reaction scheme was evident: both sor-

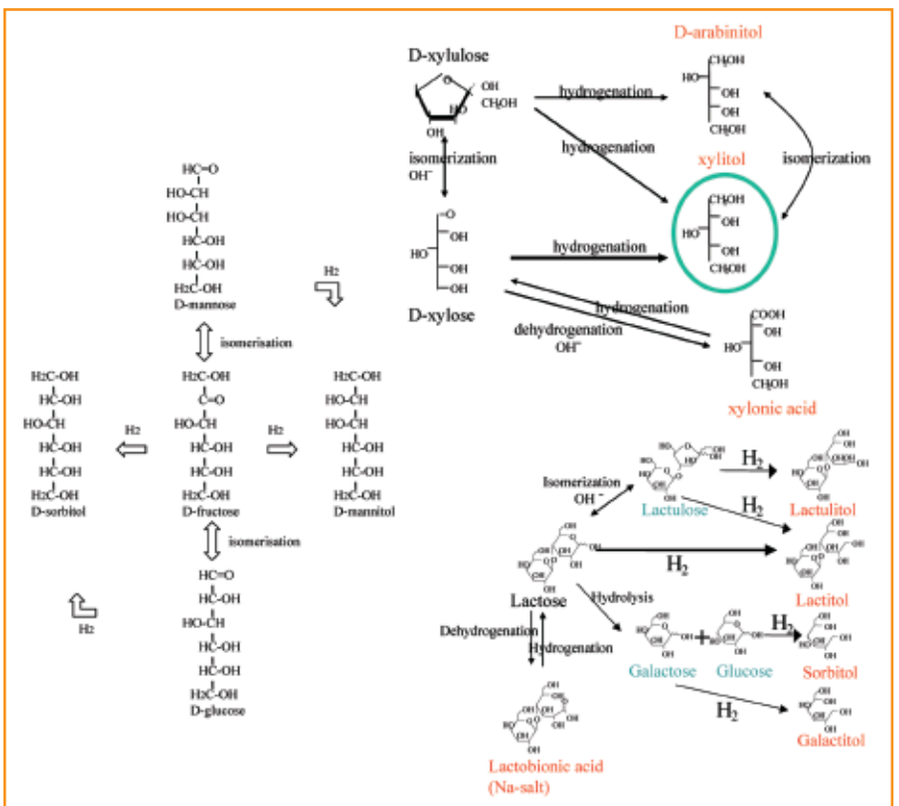

Fig. 1 - Reaction schemes for hydrogenation of *D*-fructose, *D*-xylose and *D*-lactose

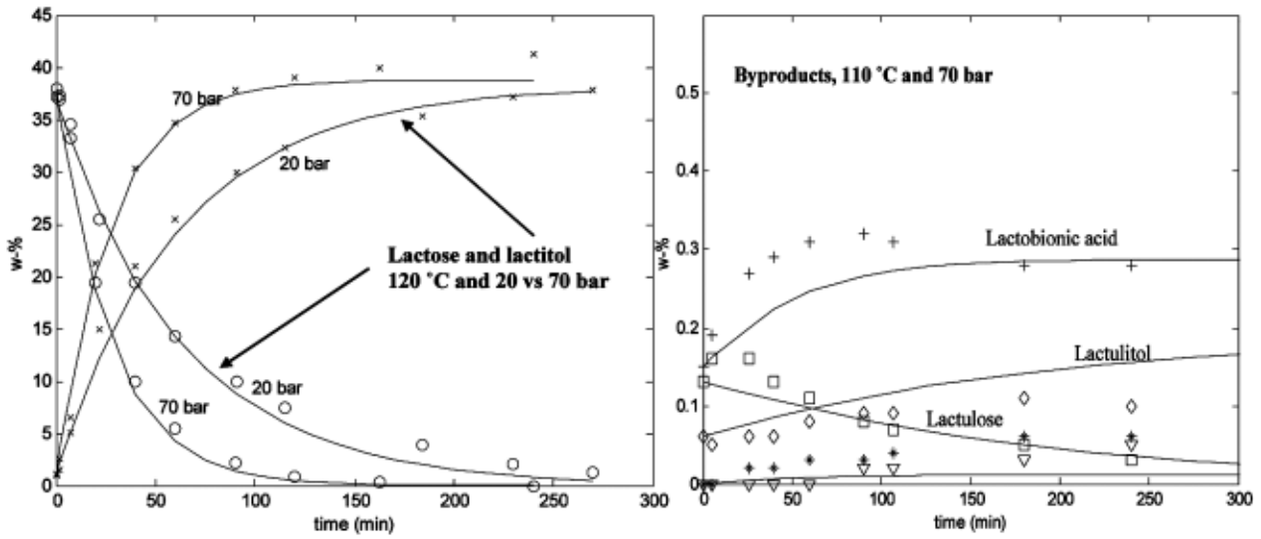

Fig. 2 - Intrinsic kinetics - hydrogenation of lactose on finely dispersed sponge Ni

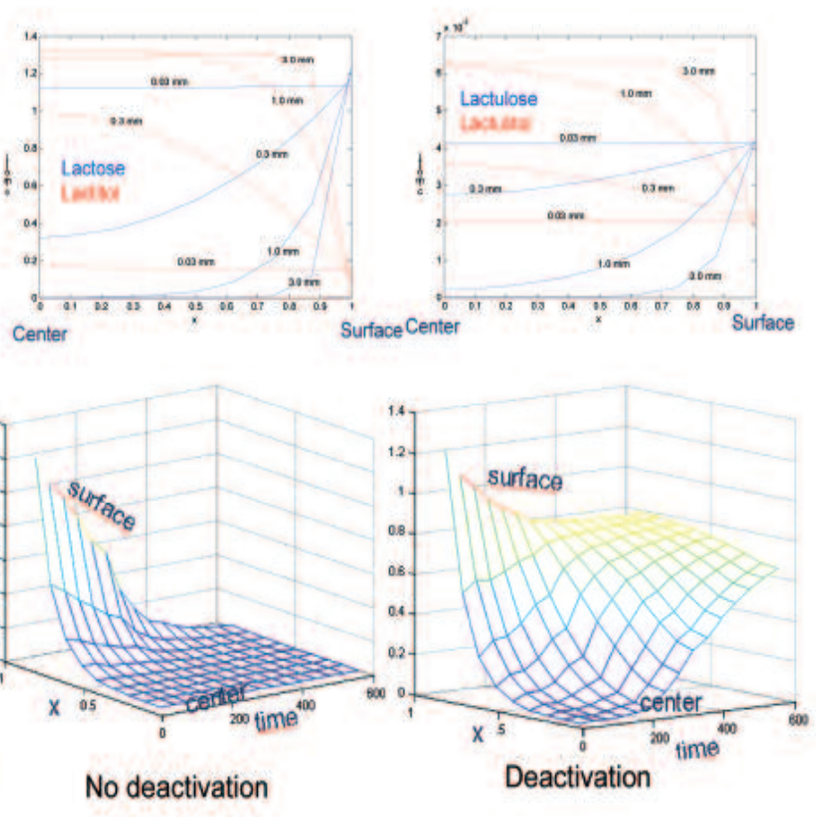

Fig. 3 - Internal mass transfer resistance and catalyst deactivation: concentration profiles inside a catalyst particle - lactose hydrogenation to lactitol and by-products

bitol and mannitol were formed, the selectivity remaining constant during the reaction.

Preliminary kinetic analysis revealed that the reactions mentioned for various sugars were close to first order with respect the organic reactant, whilst the reaction order with respect to hydrogen varied between 0.5 and 2.2, being 0.7 for hydrogenation of lactose on sponge nickel and about 2 for fructose hydrogenation on CuO/ZnO. The proposed reaction schemes are collected in Fig. 1.

Intrinsic kinetics and diffusion phenomena

Rate expressions based on the principle of an ideal surface, rapid adsorption and desorption, but rate-limiting hydrogenation steps were derived. The competitiveness of adsorption and the state of hydrogen on the catalyst surface has been the subject of intensive discussions in the literature (see e.g. [4]), but in this case we remained with the simplest possible model, non-competitive adsorption of hydrogen and organics along with molecular adsorption of hydrogen. Previous comparisons [4] have shown that this approach gives an adequate

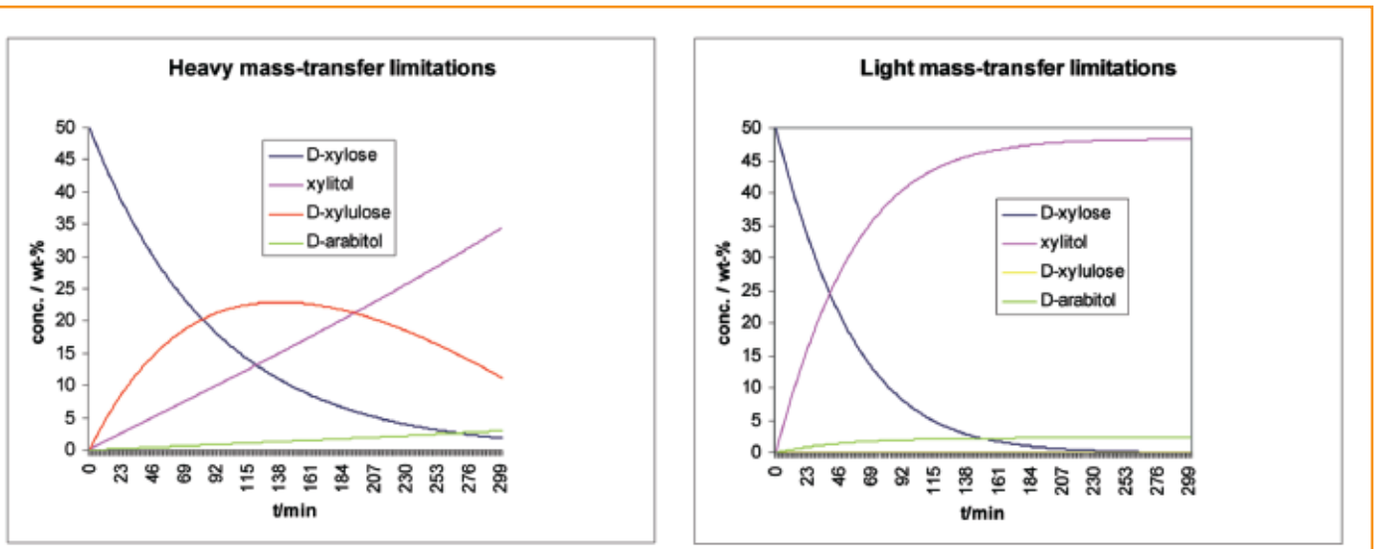

Fig. 4 - External mass transfer resistance - xylose hydrogenation to xylitol and by-products

description of the kinetics, with a minimum number of adjustable parameters. Sample fits are provided by Fig. 2. A thorough comparison of experimental data with modeling results indicated that the model for intrinsic kinetics is sufficient and can be used for simulation of the reaction-diffusion phenomena in larger catalyst particles.

Some simulation results for large catalyst particles (lactose hydrogenation) are provided by Fig. 3. As the figure reveals, the process becomes easily diffusion-limited, not only by hydrogen diffusion but also that of the organic educts and products. For particles with diameters more than 0.03 mm, diffusion resistance is visible. This is valid not only for the main components, such as lactose and lactitol, but also for by-products, such as lactulose and lactulitol. The effect of deactivation is illustrated in lower part of Fig. 3, where the concentration front moves towards the centre of the particle, since the outer layer of the particle deactivates. As the reaction progresses to high conversions, the role of diffusion resistance diminishes, because all of the reaction rates become low.

For 'small' catalyst particles used in sugar hydrogenation (slurry reactors), one would intuitively conclude that the system is safely on the kinetic regime. The simulation results obtained for sugar hydrogenation strongly suggest that this is not the case. The organic molecules are large, having molecular diffusion coefficients of the magnitude $4.0 \cdot 10^{-9}$ m^2/s. The porosity-to-tortuosity factor can be rather small (<<0.5), thus the effective diffusion coefficient becomes small, and internal diffusion resistance becomes an important factor.

In addition, external diffusion resistance is often a crucial factor in sugar hydrogenation: due to inappropriate stirrer design and high viscosity, the risk for lack of hydrogen in the liquid phase is high. A simulations of the hydrogen content in the liquid phase indicated that a complete saturation is achieved at high conversions, while the hydrogen concentration is below saturation in the beginning of the experiment. By increasing the stirring efficiency, the k_L-values can be improved and the role of external mass transfer resistance is suppressed. The hydrogen concentration in the liquid phase plays a crucially important role for the production: in the case of external mass transfer limitation of hydrogen, the isomerisation reaction yielding xylulose, which does not need any hydrogen, is favoured (Fig. 4).

Conclusions

Alternative sweeteners are produced from natural, renewable raw materials. These kind of sweeteners are not only harmless for human

Dolcificanti alternativi: la dolce vita

RIASSUNTO

In questo lavoro viene studiata l'idrogenazione catalitica in sistemi trifasici di materie prime naturali (D-fruttosio, D-xilosio e D-lattosio) per la produzione di dolcificanti. È riportato un modello matematico in grado di descrivere con successo la reazione, il trasferimento di materia e la disattivazione del catalizzatore.

health, but they possess health-promoting properties. We have presented kinetic models and general reaction-diffusion-deactivation models for porous catalyst particles in stirred semi-batch reactors applied to production of alternative sweeteners, such as mannitol, xylitol and lactitol. The case studies revealed that both internal and external resistances can considerably affect the rate and selectivity of the process. To get the best possible performance of industrial reactors, it is necessary to use this kind of simulation approach, which helps to optimize the process parameters, such as temperature, hydrogen pressure, catalyst particle size and the stirring conditions.

Acknowledgements: *This work is part of the activities at the Åbo Akademi Process Chemistry Centre within the Finnish Centre of Excellence Programmes (2000-2011) by the Academy of Finland.*

References

[1] P. Gallezot *et al., Journal of Catalysis,* 1998, **180,** 51.
[2] J. Kuusisto *et al., Industrial & Engineering Chemistry Research,* 2006, accepted.
[3] E. Santacesaria *et al., Catalysis Today,* 1999, **52,** 363.
[4] T. Salmi *et al., Industrial & Engineering Chemistry Research,* 2004, **43,** 4540.
[5] D. Murzin, T. Salmi, Catalytic Kinetics, Elsevier, Amsterdam, 2005, ISBN 0-444-51605-0.
[6] J. Kuusisto *et al., Catalysis Today,* 2006, submitted.
[7] E.W. Thiele, *Ind. Eng. Chem.,* 1939, **31,** 916.
[8] D.A. Frank-Kamenetskii, Diffusion and heat-transfer in chemical kinetics, Princeton Univ. Press, N.J., 1955.
[9] F. Sandelin *et al., Industrial & Engineering Chemistry Research,* 2006, **45,** 558.
[10] C.R. Wilke, P. Chang, *Am. Inst. Chem. Engrs J.,* 1955, **1,** 264.
[11] W. Hayduk, B.S. Minhas, *Can. J. Chem. Eng.,* 1982, **60,** 295.
[12] P.G.T. Fogg, W. Gerrard,, Solubility of gases in liquids, Wiley, Chichester, 1992.
[13] J-P. Mikkola *et al., Journal Chem. Technol. and Biotechnol.,* 1999, **74,** 655.
[14] M.I. Temkin *et al., J. Phys. B,* 1988, **21,** 1907.
[15] J. Hájek, D.Yu. Murzin, *Industrial & Engineering Chemistry Research,* 2004, **43,** 2030.
[16] A.C. Hindmarsh, ODEPACK-A Systematized Collection of ODE-Solvers, R. Stepleman *et al*., Scientific Computing, IMACS/North Holland Publishing Company, 1983, p. 55-64.

Notation

a	catalyst activity factor
a_p	catalyst particle mass transfer area to reactor volume relation
a_{GL}	gas-liquid mass transfer area to reactor volume relation
A	mass transfer area
c	concentration
d	diameter
D_e	effective diffusion coefficient
k	rate constant,
k_L, k_G	mass transfer coefficient
K	gas-liquid equilibrium constant
n	molar amount
N	flux, mol/m^{2}s
p	partial pressure
P	total pressure
r	component reaction rate
r	radius, m
R	reaction rate
R	gas constant 8.3143 J/molK
s	catalyst particle shape factor
t	time, min
x	mole fraction
ε_p	porosity
ε	specific mixing power
ρ_p	catalyst particle density
ν	kinematic viscosity
η	viscosity (in cP)
Re	Reynolds number
Sc	Schmidt number
Sh	Sherwood number

Subscripts and superscripts

b	bulk property
G	gas phase
i	component index
j	reaction index
L	liquid phase
p	catalyst particle property
*	equilibrium condition